Admittance Matrix Estimation of Radial Distribution Grids using Power and Voltage Magnitude Measurements

Mohammad Rayati, Mokhtar Bozorg
School of Engineering and Management Vaud
University of Applied Sciences and Arts Western Switzerland
Yverdon-les-Bains, Switzerland
{mohammad.rayati, mokhtar.bozorg}@heig-vd.ch

Omid Alizadeh-Mousavi
DEPsys SA
Puidoux, Switzerland

***Abstract*—Accurate knowledge of the admittance matrix of distribution grids is essential for grid operation and control as more renewable energy sources and electric vehicles are integrated into distribution grids. Due to limited observability, measurement noise, topology assumptions, and partial data availability, the exact calculation of the admittance matrix of distribution grids is challenging. In this paper, we present a method for estimating the admittance matrix of radial distribution grids. The proposed method uses low-cost measurement devices that record ten-minute-based measurements of voltage magnitudes, active power, and reactive power at a single end of the lines or transformers instead of second-based phasor measurements. The impedance of lines or transformers is then estimated using a statistical optimization subject to the distribution flow (DistFlow) model. The effectiveness of proposed method is demonstrated by simulation, laboratory testing, and field measurements taken from a distribution grid in Switzerland.**

***Index Terms*—Admittance matrix, Distribution flow (DistFlow) model, Grid-side measurement devices, Parameter estimation, Radial distribution grids.**

I. Introduction

The electrical load configuration of distribution grids is changing because more electric vehicles and heat pumps are being integrated into the demand side, and more intermittent renewable energy sources, such as photovoltaics, are being installed. These changes are directly affecting how medium-voltage (MV) and low-voltage (LV) distribution grids are operated and controlled. The recently developed operation and control algorithms for distribution grids rely on real-time monitoring of the MV and LV grids as well as knowledge of the admittance matrix, which provides details on the grid topology and the parameters of the lines and transformers [1].

There has been an effort in the literature towards estimating the admittance matrix using grid-side measurements, e.g., [2]–[8]. This effort is motivated by two major reasons: *First*, the precise and up-to-date parameters of the lines and transformers are not always available, particularly in LV distribution grids. The registered values of the line and transformer parameters may change due to aging, temperature variations, and so on. *Second*, the states of switches in LV grids, as well as the grid topology, frequently change without being precisely recorded.

The previous methods proposed for estimating the admittance matrix mostly make use of second-based data from remote terminal units (RTUs) or micro phasor measurement units (μ-PMUs). The patent [2] has described a method for real-time recursive parameter estimation of MV grids' lines and transformers depending on data recorded at RTUs. It assumes that the voltage magnitude of distribution grids follows a Gaussian probability density, which is not accurate. The patent [3] has developed a method for real-time estimation of the impedance of a length of a power line monitored at least at two different locations by μ-PMUs. A parameter estimation technique has been proposed in [4] for calculating the admittance matrix of power grids from the recorded data of μ-PMUs distributed across the grid. In [5], the method of calculating the admittance matrix has been explained and its sensitivity to the number of μ-PMUs has been studied. Though the error of admittance matrix estimation rapidly decreases with the addition of measurement devices, it has been demonstrated that the error eventually reaches a fixed value that is dependent on the measurement noise.

A method for joint identification of admittance parameters and the topology of a poly-phase distribution grid has been proposed in [6]. This method uses precise μ-PMUs installed across the grid and a sparsity-based regularization technique to improve the accuracy of the identification process. Despite the advantages of proposed method, it is vulnerable to measurement noise and the tuning of regularization parameters. It has been shown in [6] that the proposed method yields sufficiently accurate estimation in the distribution grid when the total vector error (TVE) of μ-PMUs is less than 0.01%. The paper [7] has proposed a method for estimating the parameters of admittance matrix for a generic unbalanced and untransposed three-phase distribution grid. The proposed method uses measurements of μ-PMUs and includes a cluster-averaging preprocessing step to lessen the vulnerability of

Submitted to the 23rd Power Systems Computation Conference (PSCC 2024).

the estimation results to measurement noise. Although the proposed method [7] improves the performance of admittance matrix estimation using μ-PMUs, it depends on a large number of μ-PMUs deployed on the lines as well as nodal injections. A method for identifying the topology and parameters of distribution grids using data from installed μ-PMUs across the grid has been proposed in [8]. The paper shows that the performance of the proposed admittance matrix estimation is unacceptable whenever the TVE of μ-PMUs exceeds 0.18%.

Previous studies have assumed that the voltage and current phasors are precisely measured via error-free (or low-error) μ-PMUs. Furthermore, they have assumed that several μ-PMUs are placed in desirable locations. These assumptions make it challenging to implement the developed methods practically, especially in LV grids, due to the following reasons: (i) Micro-PMUs are expensive, costing more than ten times the price of measurement devices that just record power and voltage magnitudes [9]. (ii) Micro-PMUs are not ideal and error-free. In addition, because the lines of LV grids are short, the differences between phase angles of neighboring nodes are small and can be within the range of measurement error of μ-PMUs. (iii) The number of lines and nodes in distribution grids (LV in particular) is gigantic. To properly estimate the admittance matrix, a large number of μ-PMUs must be placed if previously developed methods are to be used.

In this paper, we propose an alternative method that does not rely on the voltage and current phasor data for estimating the admittance matrix. We propose an estimation method using data coming from low-cost measurement devices that just record ten-minute three-phase voltage magnitudes, active power, and reactive power with a specified level of precision[1]. The proposed estimation method is based on the distribution flow (DistFlow) model for radial grids, and it solves a regression problem to figure out the best-fit DistFlow equations suited to the measurement data.

The paper is organized as follows: Section II presents the problem statement. Section III introduces the proposed method. Section IV presents the performance evaluation of the proposed method. Finally, Section V concludes the paper.

II. Problem Statement

We investigate the problem of estimating the parameters of the admittance matrix of a three-phase radial distribution grid, given the following assumptions: (i) The grid topology is known using other approaches, such as the one proposed in [10] and the references therein; (ii) The power flows of distribution grids are decoupled into positive, negative, and zero sequences[2]; and (iii) A number of low-cost measurement devices are installed in specified locations to record ten-minute data with a certain level of precision, including phase-to-ground nodal voltage magnitudes as well as the active and reactive power of lines or transformers per phase. The locations of measurement devices under consideration are depicted in Fig. 1. As demonstrated, the number of measurement devices in our approach is fewer[3] than in earlier studies, i.e., [2]–[8].

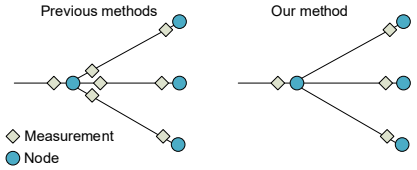

Fig. 1. Comparison of required measurement devices in our method and earlier ones.

In the following, we provide the grid model and notations that will be used to describe the admittance matrix estimation problem.

Consider a three-phase radial distribution grid with N+1 nodes. The nodes are indexed by $n \in \mathcal{N}$, the phases are indexed by $\phi \in \Phi$, and the sequence components are indexed by $s \in \mathcal{S}$, where $\mathcal{N} := \{0, 1, 2, \ldots, N\}$ is the set of nodes, $\Phi := \{a, b, c\}$ is the set of phases, and $\mathcal{S} := \{\text{zero}, \text{pos}, \text{neg}\}$ is the set of sequence components. The node $n = 0$ is the point of common coupling. For other $n \in \mathcal{L} := \mathcal{N} \setminus \{0\}$, there is a three-phase line n or a transformer n that links the node n to its upper node, i.e., $\text{up}(n) \in \mathcal{N} \setminus \{n\}$. The non-fixed-point operator $\text{up}(.) : \mathcal{L} \to \mathcal{N}$ maps each node to its upper node and determines the distribution grid topology. This function is assumed to be known.

The actual per-unit resistance and the per-unit reactance of the link connecting node $n \in \mathcal{L}$ to $\text{up}(n)$ in the sequence $s \in \mathcal{S}$ are denoted by $r_{\text{n}}^{(\text{s})}$ and $x_{\text{n}}^{(\text{s})}$, respectively. Theses parameters $(r_{\text{n}}^{(\text{s})})_{n\in\mathcal{L},s\in\mathcal{S}}$ and $(x_{\text{n}}^{(\text{s})})_{n\in\mathcal{L},s\in\mathcal{S}}$ are unknown (or outdated and potentially inaccurate). The objective of this study is to estimate them and build the admittance matrices of different sequences given the grid topology. The admittance matrix of the sequence $s \in \mathcal{S}$ of the grid is represented by $\mathbf{Y}_{\text{s}} =: [y_{\text{n,n}'}^{(\text{s})}]_{(N+1)\times(N+1)}$, in which

$$y_{\text{n,n}'}^{(\text{s})} = \begin{cases} -1/(r_{\text{n}}^{(\text{s})} + j \cdot x_{\text{n}}^{(\text{s})}) & \text{if } n' = \text{up}(n), \\ -1/(r_{\text{n}'}^{(\text{s})} + j \cdot x_{\text{n}'}^{(\text{s})}) & \text{if } n' \in \mathcal{DN}_{\text{n}}, \\ \sum\limits_{n''\in(\mathcal{DN}_{\text{n}}\cup\{n\})} \left(\frac{1}{r_{\text{n}''}^{(\text{s})} + j \cdot x_{\text{n}''}^{(\text{s})}} \right) & \text{if } n' = n, \\ 0 & \text{otherwise,} \end{cases} \tag{1}$$

where $\mathcal{DN}_{\text{n}} =: \{n' \mid \text{up}(n') = n\}$ is the set of the nodes down below the node $n \in \mathcal{N}$. Note that $2 \times (N + 1)$ components of the matrix $\mathbf{Y}_{\text{s}}$ are non-zero out of $(N + 1)^2$ components. Thus, the matrix $\mathbf{Y}_{\text{s}}$ is sparse. Furthermore, the matrix $\mathbf{Y}_{\text{s}}$ is symmetric and singular by definition.

Let $V_{\text{n,t}}^{(\phi)}$ be the per-unit line-to-ground voltage phasor of node $n \in \mathcal{N}$ and phase $\phi \in \Phi$ at time $t \in \mathcal{T}$, where

[1] In [9], the absolute impedances of lines and transformers were estimated using data from low-cost measurement devices. In this paper, we will investigate estimating the resistance and reactance values. It should be noted that we will not investigate estimating the transversal elements (specifically, the line capacitance).

[2] When the grid is symmetrical, i.e., the mutual inductance between each pair of phases is equal, and the sequence components (positive, negative, and zero) are independent.

[3] For a radial grid with N+1 nodes, our approach needs N+1 low-cost measurement devices, whereas earlier methods need $2\times N$ μ-PMUs.

$\mathcal{T} := \{1, 2, \ldots, T\}$ is the set of sampled measurements. Furthermore, let $I^{(\phi)}_{\mathrm{n,n',t}}$ be the per-unit flowing current phasor from node $n \in \mathcal{N}$ to node $n' \in \mathcal{DN}_{\mathrm{n}} \cup \{\mathrm{up}(n)\}$ of phase $\phi \in \Phi$ at time $t \in \mathcal{T}$. Note that the voltage and current might be unbalanced. Using the method of symmetrical components, the sequential voltage and current for all $n \in \mathcal{N}$, $n' \in \mathcal{DN}_{\mathrm{n}} \cup \{\mathrm{up}(n)\}$, and $t \in \mathcal{T}$ are

$$\mathrm{col}_{s\in\mathcal{S}}(V^{(\mathrm{s})}_{\mathrm{n,t}}) := \mathbf{A^{-1}} \cdot \mathrm{col}_{\phi\in\Phi}(V^{(\phi)}_{\mathrm{n,t}}), \tag{2}$$

$$\mathrm{col}_{s\in\mathcal{S}}(I^{(\mathrm{s})}_{\mathrm{n,n',t}}) := \mathbf{A^{-1}} \cdot \mathrm{col}_{\phi\in\Phi}(I^{(\phi)}_{\mathrm{n,n',t}}), \tag{3}$$

where the operator "col(.)" constructs a column vector, $\mathbf{A^{-1}} := \frac{1}{3} \cdot [[1,1,1]^\top, [1,\alpha,\alpha^2]^\top, [1,\alpha^2,\alpha]^\top]$ is the transformation matrix, $(.)^\top$ denotes the transpose operator, and $\alpha := \exp^{\frac{2}{3}\cdot\pi\cdot j}$ is the phasor rotation operator [11].

The flowing active power and reactive power of different sequences[4] are computed for all $n \in \mathcal{N}$, $n' \in \mathcal{DN}_{\mathrm{n}} \cup \{\mathrm{up}(n)\}$, $t \in \mathcal{T}$, and $s \in \mathcal{S}$ by $P^{(\mathrm{s})}_{\mathrm{n,n',t}} := \Re(V^{(\mathrm{s})}_{\mathrm{n,t}} \cdot (I^{(\mathrm{s})}_{\mathrm{n,n',t}})^\dagger)$ and $Q^{(\mathrm{s})}_{\mathrm{n,n',t}} := \Im(V^{(\mathrm{s})}_{\mathrm{n,t}} \cdot (I^{(\mathrm{s})}_{\mathrm{n,n',t}})^\dagger)$, where $(.)^\dagger$ is the complex conjugate operator, $\Re(.)$ refers the real part, and $\Im(.)$ refers to the imaginary part of a complex quantity. We represent the voltage matrix of sequence $s \in \mathcal{S}$ by $\mathbf{V}_{\mathrm{s}} := [V^{(\mathrm{s})}_{\mathrm{n,t}}]_{(N+1)\times T}$. In addition, we define the flowing active and reactive power matrices as $\mathbf{P}_{\mathrm{s}} := [P^{(\mathrm{s})}_{\mathrm{n,up(n),t}}]_{N\times T}$, $\mathbf{Q}_{\mathrm{s}} := [Q^{(\mathrm{s})}_{\mathrm{n,up(n),t}}]_{N\times T}$, $\mathbf{P}^{(\mathrm{up})}_{\mathrm{s}} := [P^{(\mathrm{s})}_{\mathrm{up(n),n,t}}]_{N\times T}$, and $\mathbf{Q}^{(\mathrm{up})}_{\mathrm{s}} := [Q^{(\mathrm{s})}_{\mathrm{up(n),n,t}}]_{N\times T}$. Then, the injected active power and reactive power matrices are calculated by $\mathbf{P}^{(\mathrm{inj})}_{\mathrm{s}} := \mathbf{P}_{\mathrm{s}} + \mathbf{B} \cdot \mathbf{P}^{(\mathrm{up})}_{\mathrm{s}}$ and $\mathbf{Q}^{(\mathrm{inj})}_{\mathrm{s}} := \mathbf{Q}_{\mathrm{s}} + \mathbf{B} \cdot \mathbf{Q}^{(\mathrm{up})}_{\mathrm{s}}$, where the matrix $\mathbf{B} := [b_{\mathrm{n,n'}}]_{N\times N}$ is used to calculate the injected power at each node, in which

$$b_{\mathrm{n,n'}} = \begin{cases} 1 & \text{if } n = \mathrm{up}(n'), \\ 0 & \text{otherwise.} \end{cases} \tag{4}$$

If the matrices $\mathbf{V}_{\mathrm{s}}$, $\mathbf{P}^{(\mathrm{inj})}_{\mathrm{s}}$, and $\mathbf{Q}^{(\mathrm{inj})}_{\mathrm{s}}$ are known, $\mathbf{Y}_{\mathrm{s}}$ can be theoretically estimated by solving the following optimization problem (see [4], [5] for developed methods to solve (5)).

$$\min_{\mathbf{Y}_{\mathrm{s}}\in\mathbb{C}^{(N+1)\cdot(N+1)}} \|\mathbf{P}^{(\mathrm{inj})}_{\mathrm{s}} + j \cdot \mathbf{Q}^{(\mathrm{inj})}_{\mathrm{s}} - \mathbf{V}_{\mathrm{s}} \cdot \mathbf{V}_{\mathrm{s}}{}^{\mathsf{H}} \cdot \mathbf{Y}_{\mathrm{s}}{}^{\mathsf{H}}\|_F \tag{5}$$
$$\text{s.t.: (1),}$$

where $\mathbb{C}$ is the complex space and $||.||_F$ represents the Frobenius norm[5].

One of the main challenges to formulating and solving (5) is that the voltage and current phasors of all nodes and phases must be measured with sufficient precision (specifically, the differences in phase angles of neighboring nodes). Due to the excessively short length of the lines in distribution grids, the phase angle differences between neighboring nodes are small. Therefore, (5) cannot provide us with a reliable result, as shown in Section IV. In this paper, we propose an alternative method that does not rely on precise measurements of all nodes' voltage and current phasors.

[4]The active and reactive power flow might also be unbalanced, resulting in non-negative values across negative and zero sequences.

[5]The Frobenius norm of a matrix $\mathbf{A} = [a_{\mathrm{i,j}}]$ is $\|\mathbf{A}\|_F := \sqrt{\sum_{i,j} |a_{\mathrm{i,j}}|^2}$.

III. Proposed Method

The proposed method relies on the DistFlow model, which is a load-flow model that does not depend on the nodal phase angles and is extensively well-suited in applications such as optimal power flow and grid planning in radial distribution grids [12]. The DistFlow model is an iterative approach consisting of a *"backward"* and *"forward"* swipe on a tree with the aim of determining the state of the grid using the inputs of active and reactive power of loads and the voltage in the slack node. The equation of the *"forward"* swipe of the DistFlow model in matrix form is

$$2 \cdot \mathbf{R}_{\mathrm{s}} \cdot \mathbf{P}_{\mathrm{s}} + 2 \cdot \mathbf{X}_{\mathrm{s}} \cdot \mathbf{Q}_{\mathrm{s}} - \mathbf{Z}_{\mathrm{s}} \cdot \mathbf{L}_{\mathrm{s}} = \mathbf{M} \cdot \mathbf{U}_{\mathrm{s}}, \tag{6}$$

where $\mathbf{R}_{\mathrm{s}} := \mathrm{diag}_{n\in\mathcal{L}}(r^{(\mathrm{s})}_{\mathrm{n}})$ and $\mathbf{X}_{\mathrm{s}} := \mathrm{diag}_{n\in\mathcal{L}}(x^{(\mathrm{s})}_{\mathrm{n}})$ are resistance and reactance matrices, $\mathbf{U}_{\mathrm{s}} := \mathbf{V}_{\mathrm{s}} \odot \mathbf{V}_{\mathrm{s}}$ is the squared voltage magnitude matrix,

$$\mathbf{Z}_{\mathrm{s}} := \mathbf{R}_{\mathrm{s}} \cdot \mathbf{R}_{\mathrm{s}} + \mathbf{X}_{\mathrm{s}} \cdot \mathbf{X}_{\mathrm{s}}, \tag{7}$$

is the squared impedance matrix,

$$\mathbf{L}_{\mathrm{s}} := (\mathbf{P}_{\mathrm{s}} \odot \mathbf{P}_{\mathrm{s}} + \mathbf{Q}_{\mathrm{s}} \odot \mathbf{Q}_{\mathrm{s}}) \oslash (\mathbf{J} \cdot \mathbf{U}_{\mathrm{s}}), \tag{8}$$

is the squared current matrix, $\mathbf{J} := [\mathrm{col}_{n\in\mathcal{L}}(0), \mathrm{diag}_{n\in\mathcal{L}}(1)]$ is a semi-identity matrix, $\odot$ denotes the Hadamard product (i.e., element-wise product), $\oslash$ denotes the Hadamard division (i.e., element-wise division), and $\mathbf{M} := [m_{\mathrm{n,n'}}]_{N\times(N+1)}$ denotes the incidence matrix, in which

$$m_{\mathrm{n,n'}} = \begin{cases} -1 & \text{if } n' = \mathrm{up}(n), \\ 1 & \text{if } n' = n, \\ 0 & \text{otherwise.} \end{cases} \tag{9}$$

If the matrices $\mathbf{U}_{\mathrm{s}}$, $\mathbf{P}_{\mathrm{s}}$, $\mathbf{Q}_{\mathrm{s}}$, and $\mathbf{M}$ are known, then $\mathbf{R}_{\mathrm{s}}$ and $\mathbf{X}_{\mathrm{s}}$ can be theoretically estimated by solving the following optimization problem:

$$\min_{\mathbf{R}_{\mathrm{s}},\mathbf{X}_{\mathrm{s}}} \|\mathbf{R}_{\mathrm{s}} \cdot \mathbf{P}_{\mathrm{s}} + \mathbf{X}_{\mathrm{s}} \cdot \mathbf{Q}_{\mathrm{s}} - \frac{\mathbf{Z}_{\mathrm{s}} \cdot \mathbf{L}_{\mathrm{s}}}{2} - \frac{\mathbf{M} \cdot \mathbf{U}_{\mathrm{s}}}{2}\|_F \tag{10}$$
$$\text{s.t.: (7), (9),}$$
$$\mathbf{R}_{\mathrm{s}} = \mathrm{diag}_{n\in\mathcal{L}}(r^{(\mathrm{s})}_{\mathrm{n}}) \in \mathbb{R}^{N\cdot N}_{\geq}, \tag{11}$$
$$\mathbf{X}_{\mathrm{s}} = \mathrm{diag}_{n\in\mathcal{L}}(x^{(\mathrm{s})}_{\mathrm{n}}) \in \mathbb{R}^{N\cdot N}_{\geq}, \tag{12}$$

where $\mathbb{R}_{\geq}$ is the set of non-negative real numbers.

The problem (10) is a quadratic programming problem that can be solved by off-the-shelf optimization solvers, e.g., CPLEX [13] or SLSQP [14]. However, there are two difficulties when dealing with the problem (10). *First*, the matrices $\mathbf{U}_{\mathrm{s}}$, $\mathbf{P}_{\mathrm{s}}$, and $\mathbf{Q}_{\mathrm{s}}$ cannot be directly determined by measuring three-phase nodal voltage magnitudes, active power, and reactive power. *Second*, there is a numerical issue in (10) resulting in non-accurate solutions. The numerical issue arises from the fact that for every $n \in \mathcal{L}$, $t \in \mathcal{T}$, and $s \in \mathcal{S}$ in a distribution grid, there is a high probability that $Q^{(\mathrm{s})}_{\mathrm{n,t}} \ll P^{(\mathrm{s})}_{\mathrm{n,t}}$ and the value of $V^{(\mathrm{s})}_{\mathrm{n,t}}$ does not fluctuate greatly. As a result, the matrices $\mathbf{P}_{\mathrm{s}}$ and $\mathbf{L}_{\mathrm{s}}$ in (10) are near-linearly dependent and as seen in Fig. 2 the optimization solvers converge to a

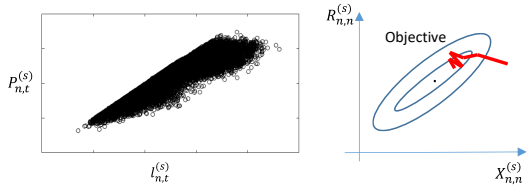

Fig. 2. Near-linearly dependency of $\mathbf{P}_{\mathrm{s}}$ and $\mathbf{L}_{\mathrm{s}}$.

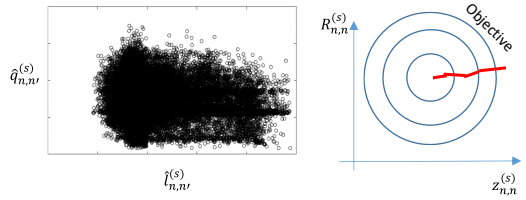

Fig. 3. Independency of $\hat{\mathbf{q}}_{\mathrm{s,k}}$ and $\hat{\mathbf{l}}_{\mathrm{s,k}}$.

non-accurate solution because the sensitivity of the solution to measurement noise is not negligible.

To tackle the aforementioned difficulties for solving (10), a step-by-step summary of the proposed method is provided in Table I. The remainder of this section explains each step of the proposed method in detail.

(i) Approximating sequential magnitudes: In our proposed method, we merely measure the three-phase magnitudes of voltage, active power, and reactive power; however, we require their sequential magnitudes to estimate $\mathbf{Y}_{\mathrm{s}}$ for all sequences $s \in \mathcal{S}$. Without exact measurement of the voltage angle of each phase, we assume that the voltage angles of the three phases are symmetrically distributed and that the phasor rotations, denoted by α_{a}, α_{b}, and α_{c}, are 1, α^2, and α, respectively. Then, the approximated voltage phasor of node n will be $\widetilde{V}^{(\phi)}_{\mathrm{n,t}} = |V^{(\phi)}_{\mathrm{n,t}}| \cdot \alpha_\phi$. We estimate the current phasors by $\tilde{I}^{(\phi)}_{\mathrm{n,t}} = \left(\frac{P^{(\phi)}_{\mathrm{n,t}} + j \cdot Q^{(\phi)}_{\mathrm{n,t}}}{\tilde{V}^{(\phi)}_{\mathrm{n,t}}}\right)^{\dagger}$. Using (2) and (3), the voltage and current phasors of different sequences are estimated. The active power and reactive power of different sequences are calculated by $\widetilde{P}^{(\mathrm{s})}_{\mathrm{n,t}} := \Re(\widetilde{V}^{(\mathrm{s})}_{\mathrm{n,t}} \cdot (\tilde{I}^{(\mathrm{s})}_{\mathrm{n,t}})^{\dagger})$ and $\widetilde{Q}^{(\mathrm{s})}_{\mathrm{n,t}} := \Im(\widetilde{V}^{(\mathrm{s})}_{\mathrm{n,t}} \cdot (\tilde{I}^{(\mathrm{s})}_{\mathrm{n,t}})^{\dagger})$.

(ii) Removing outliers: The extreme data points are transformed into z-scores, which indicate how much they deviate from the mean. We eliminate any time steps $t \in \mathcal{T}_{\mathrm{ol}}$ with a z-score of greater than 3 or below -3. We also eliminate the time steps $t \in \mathcal{T}_{\mathrm{zero}}$ that the active power and voltage magnitude are less than the predetermined values ϵ_{p} and ϵ_{v}. The set $\mathcal{T}' = \mathcal{T} \setminus (\mathcal{T}_{\mathrm{ol}} \cup \mathcal{T}_{\mathrm{zero}})$ is the set of regular data points.

(iii) Sampling with replacement: To ensure an unbiased estimation, we run the proposed algorithm multiple times rather than once with all samples, i.e., regular data points $t \in \mathcal{T}'$. Each time, we select a random subset of the regular data points. Then, we run the estimation algorithm on that random subset. The term "*test*" refers to each execution of the estimation algorithm on a randomly selected subset of regular data points. Let K represent the total number of tests, and T_{k} represent the total number of samples used in the test k. We choose at random T_{k} time steps from the set $\mathcal{T}'$. The set of random time steps is called as $\mathcal{T}_{\mathrm{k}}$. Then, we establish the matrices $\hat{\mathbf{P}}_{\mathrm{s,k}} := [\mathrm{col}_{n\in\mathcal{L}}(\mathrm{col}_{t\in\mathcal{T}_k}(\tilde{P}^{(\mathrm{s})}_{\mathrm{n,t}})^{\top})]$, $\hat{\mathbf{Q}}_{\mathrm{s,k}} := [\mathrm{col}_{n\in\mathcal{L}}(\mathrm{col}_{t\in\mathcal{T}_k}(\tilde{Q}^{(\mathrm{s})}_{\mathrm{n,t}})^{\top})]$, $\hat{\mathbf{V}}_{\mathrm{s,k}} := [\mathrm{col}_{n\in\mathcal{N}}(\mathrm{col}_{t\in\mathcal{T}_k}(\tilde{V}^{(\mathrm{s})}_{\mathrm{n,t}})^{\top})]$, $\hat{\mathbf{U}}_{\mathrm{s,k}} := \hat{\mathbf{V}}_{\mathrm{s,k}} \odot \hat{\mathbf{V}}_{\mathrm{s,k}}$, and

TABLE I
PROPOSED METHOD FOR ESTIMATING $(\mathbf{Y}_{\mathrm{s}})_{s\in\mathcal{S}}$.

(i): Approximate the magnitudes of the sequential nodal voltage, active power, and reactive power.
Run the following for all $s \in \mathcal{S}$:
(ii): Remove outliers and time steps with active power and voltage magnitude smaller than ϵ_{p} and ϵ_{v}, respectively.
Run the following for all tests $k \in \{1, 2, \ldots, K\}$:
(iii): Choose at random T_{k} time steps for the test k .
(iv): Normalize the feature matrices and solve (13).
(v): Estimate the value of $\mathbf{Y}_{\mathrm{s}}$ using (16).

$$\hat{\mathbf{L}}_{\mathrm{s,k}} := (\hat{\mathbf{P}}_{\mathrm{s,k}} \odot \hat{\mathbf{P}}_{\mathrm{s,k}} + \hat{\mathbf{Q}}_{\mathrm{s,k}} \odot \hat{\mathbf{Q}}_{\mathrm{s,k}}) \oslash (\mathbf{J} \cdot \hat{\mathbf{U}}_{\mathrm{s,k}}).$$

(iv) Normalization: To eliminate the nearly linear dependence between $\mathbf{P}_{\mathrm{s}}$ and $\mathbf{L}_{\mathrm{s}}$ in the *"forward"* swipe of the DistFlow model, i.e., in (6), we normalize the left and right-hand sides of (6) by active power. Since the resulted parameters will be independent (as illustrated in Fig. 3), we will be able to solve the following optimization problem in the test k without any numerical difficulty.

$$\min_{\mathbf{R}_{\mathrm{s}},\mathbf{X}_{\mathrm{s}}} \|\mathbf{R}_{\mathrm{s}} \cdot \mathbb{1} + \mathbf{X}_{\mathrm{s}} \cdot \hat{\mathbf{q}}_{\mathrm{s,k}} - \frac{\mathbf{Z}_{\mathrm{s}} \cdot \hat{\mathbf{l}}_{\mathrm{s,k}}}{2} - \frac{\mathbf{M} \cdot \hat{\mathbf{u}}_{\mathrm{s,k}}}{2}\|_F \tag{13}$$

$$\text{s.t.: } (7),\ (9),$$

$$\mathbf{R}_{\mathrm{s}} = \mathrm{diag}_{n\in\mathcal{L}}(r^{(\mathrm{s})}_{\mathrm{n}}) \in \mathbb{R}^{N\cdot N}_{\geq\epsilon}, \tag{14}$$

$$\mathbf{X}_{\mathrm{s}} = \mathrm{diag}_{n\in\mathcal{L}}(x^{(\mathrm{s})}_{\mathrm{n}}) \in \mathbb{R}^{N\cdot N}_{\geq\epsilon}, \tag{15}$$

where $\mathbb{R}_{\geq\epsilon} := [\epsilon, \infty)$ is the set of positive numbers bigger than or equal to $\epsilon > 0$ and $\mathbb{1} := [1]_{N\times T_{\mathrm{k}}}$ is a matrix whose elements are all equal to one. Furthermore, $\hat{\mathbf{q}}_{\mathrm{s,k}} := \hat{\mathbf{Q}}_{\mathrm{s,k}} \oslash \hat{\mathbf{P}}_{\mathrm{s,k}}$, $\hat{\mathbf{l}}_{\mathrm{s,k}} := \hat{\mathbf{L}}_{\mathrm{s,k}} \oslash \hat{\mathbf{P}}_{\mathrm{s,k}}$, and $\hat{\mathbf{u}}_{\mathrm{s,k}} := \hat{\mathbf{U}}_{\mathrm{s,k}} \oslash \hat{\mathbf{P}}_{\mathrm{s,k}}$ are the normalized reactive power, the normalized squared current, and the normalized squared voltage matrices, respectively. Note that $\mathbb{R}_{\geq}$ is substituted by $\mathbb{R}_{\geq\epsilon}$ in (14) and (15) to arrive at a non-zero solution. The set $\mathbb{R}_{\geq\epsilon}$ approximates the set of positive real numbers when ϵ is a small number, e.g., 10^{-6}. This approximation makes it possible for the optimization solvers like SLSQP to address the problem (13).

(v) Calculation of admittance matrix: Let $\mathbf{R}^*_{\mathrm{s,k}}$ and $\mathbf{X}^*_{\mathrm{s,k}}$ be the solutions of the problem (13) in the test k. The resistance and reactance matrices are estimated by $\mathbf{R}^*_{\mathrm{s}} := \frac{1}{K} \cdot \sum_{k=1}^{K} \mathbf{R}^*_{\mathrm{s,k}}$ and $\mathbf{X}^*_{\mathrm{s}} := \frac{1}{K} \cdot \sum_{k=1}^{K} \mathbf{X}^*_{\mathrm{s,k}}$. Then, the admittance matrix is calculated by,

$$\mathbf{Y}^*_{\mathrm{s}} = \mathbf{M}^{\top} \cdot (\mathrm{diag}_{n\in\mathcal{L}}(1) \oslash (\mathbf{R}^*_{\mathrm{s}} + j\mathbf{X}^*_{\mathrm{s}})) \cdot \mathbf{M}. \tag{16}$$

IV. Performance Evaluation

The proposed method is validated in three cases: *"SYN"*, *"LAB"*, and *"REAL"*. In the case *"SYN"*, the proposed method is validated by synthesized data collected from simulation. In the case *"LAB"*, the proposed method is validated using data collected by the low-cost measurement devices installed in the smart grid laboratory [15]. In the case *"REAL"*, the proposed method is validated via data collected from a real-world distribution grid in Switzerland.

Two different grids are used in the three mentioned cases: the first in the "SYN" and "LAB" cases, and the second in the "REAL" case. Both grids, depicted in Figs. 4 and 5, are three-phase radial distribution grids (230/400 V, 50Hz). Tables II and III summarize the lines nominal parameters in the first and second grids, respectively.

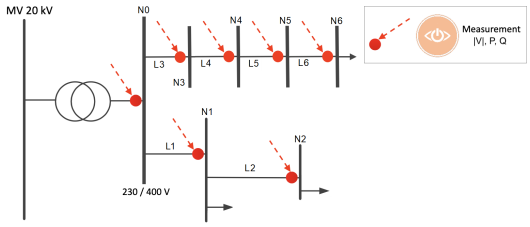

Fig. 4. First grid: used in the cases "SYN" and "LAB".

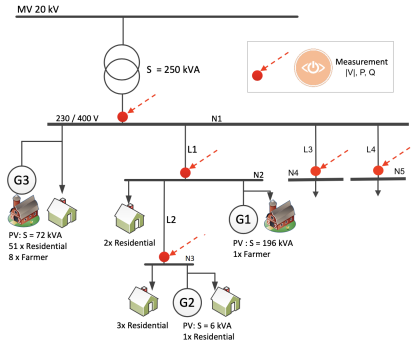

Fig. 5. Second grid: used in the case "REAL".

TABLE II
Lines nominal parameters of the first grid (Fig. 4).

	Cable type	$\hat{r}_{\mathrm{n}}^{(\mathrm{pos})}$ (Ohm)*	$\hat{x}_{\mathrm{n}}^{(\mathrm{pos})}$ (Ohm)*
L1	EPR-PUR 5x70 + adjustable $\hat{r}$ and $\hat{x}$	0.086	0.074
L2	EPR-PUR 5x70 + adjustable $\hat{r}$ and $\hat{x}$	0.064	0.063
L3	EPR-PUR 5x70 + adjustable $\hat{r}$ and $\hat{x}$	0.086	0.061
L4	EPR-PUR 5x70 + adjustable $\hat{r}$ and $\hat{x}$	0.109	0.074
L5	EPR-PUR 5x70 + adjustable $\hat{r}$ and $\hat{x}$	0.048	0.065
L6	EPR-PUR 5x70 + adjustable $\hat{r}$ and $\hat{x}$	0.109	0.071

* $\hat{r}_{\mathrm{n}}^{(\mathrm{pos})}$ and $\hat{x}_{\mathrm{n}}^{(\mathrm{pos})}$ denote the nominal resistance and reactance in Ohm.

TABLE III
Lines nominal parameters of the second grid (Fig. 5).

	Cable type	Length	$\hat{r}_{\mathrm{n}}^{(\mathrm{pos})}$ (Ohm)	$\hat{x}_{\mathrm{n}}^{(\mathrm{pos})}$ (Ohm)
L1	1kV 240mm2 AL	219m	0.021	0.016
L2	1kV 150mm2 AL	145m	0.038	0.012
L3	1kV 150mm2 AL	293m	0.078	0.024
L4	1kV 185mm2 AL	85m	0.014	0.006

The first and second grids are equipped with 7 and 5 low-cost measurement devices called GridEye[6], respectively. With a high sampling frequency, these devices record the voltage and input current at each grid node for each of the three phases. Following the acquisition, the measured quantities are post-processed to allow the computation of the average active and reactive power as well as the average voltage magnitudes. The standard deviations of measurement error of the voltage, active power, and reactive power are 0.1%, 1.0%, 1.0%, respectively.

The proposed method, including data collection and analysis, is implemented in Python. All of the Python codes for simulation, collection of data, and analysis of data in the three cases mentioned are publicly available in [17].

A. Performance Assessment: First Case "SYN"

Consider replacing the installed measurement devices in Fig. 4 with μ-PMUs that measure the flowing power of both sides of the lines. The problem (5) is solved for two sets of data, each of which is generated by simulation with the TVE of installed μ-PMUs set to 0.002% and 0.02%[7]. To simulate different TVEs of μ-PMUs, the added noises are assumed to be normal Gaussian distributed. The estimated admittance matrices are compared to the actual ones calculated from actual resistance and reactance values (using (1) and data from Table II). The absolute differences in admittance matrices are depicted in Fig. 6. When the TVEs are increased, the error of admittance matrix estimation increases significantly and raises up to 30%. Therefore, the methods relying on μ-PMUs data and their provided phase angles for estimating admittance matrix are prone to large errors. The proposed method of this paper does not rely on phase angles.

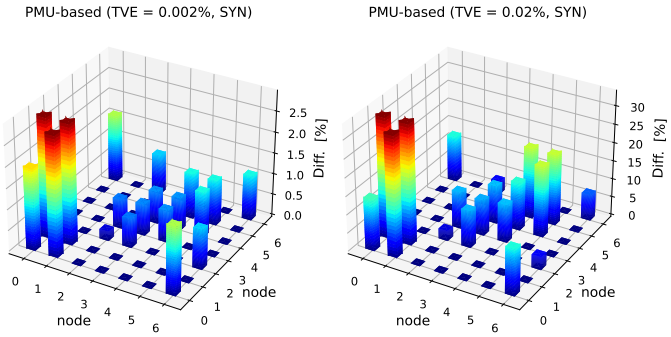

Fig. 6. Absolute differences between the actual admittance matrix and the estimated ones by problem (5) in simulation.

The absolute differences between the actual admittance matrix and the estimated ones are shown in Fig. 7 when the low-cost measurement devices are installed in the grid and the proposed method is employed. With simulation, two sets of data are generated, assuming that the error in measuring voltage magnitudes is 0.02% and 0.1%. By comparing Figs. 6 and 7, we observe that the proposed method is effective since the error in estimating the admittance matrix using the proposed method is insensitive to measurement errors and negligible.

[6]The measurement devices are developed by the DEPsys SA [16].

[7]The TVE is mathematically defined as $\mathrm{TVE} = \frac{||V_{\mathrm{m}} - \hat{V}||}{\hat{V}} \times 100\%$, where V_{m} is the measured phasor vector, $\hat{V}$ is the actual phasor vector, and $||.||$ denotes the Euclidean norm. The TVE of μ-PMUs available on the market is around 0.02% [7].

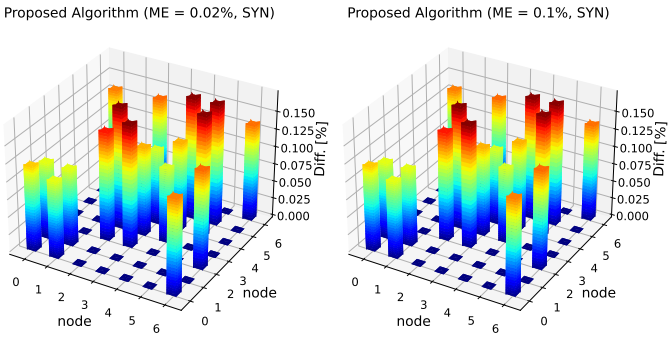

Fig. 7. Absolute differences between the actual admittance matrix and the estimated ones by proposed method in simulation.

B. Performance Assessment: Second Case "LAB"

The grid in Fig. 4 and the parameters in Table II are emulated within the ReIne laboratory. The ReIne[8] has been built at the HEIG-VD to study and plan distribution grid changes [15]. ReIne is a hardware and software platform that fully mimics a wide range of LV grid topologies as well as MV grid topologies on a per-unit basis. The flexibility of this laboratory, which uses both lumped grid elements and actual electrical sources and end-users, distinguishes it from other existing structures, e.g., [18], [19].

The ReIne is composed of a switchboard cabinet that connects production, passive and active end-users, and bidirectional power electronics converters. The grid-emulating section of the laboratory is made up of nine lines arranged in a matrix with variable resistances and inductances. The resistance-to-inductance ratios can be adjusted from 0.3 to 3.5, which represent most of the real-world MV and LV distribution grids. Two adaptive 50 kW power electronic converters, built in-house and capable of consuming and generating variable active and reactive power, also emulate different load time series.

In the locations of nodes N2 and N6 (Fig. 4), ten days of loading values are emulated. Using the measured data and solving the problem (13), the estimated resistance and reactance of positive sequences are as shown in Table IV. The difference between the estimated and the actual admittance matrices is depicted in Fig. 8. In addition, the column "*diff*" of Table IV shows the difference between estimated values and actual resistance and reactance values. Although the differences are acceptable, the differences are due to the following reasons: *First*, the measurement devices consume a load that is not measured on their own. This load is comparable to the actual loading value during low load periods, which causes the estimated line parameters to change[9]. *Second*, the accuracy of estimating the reactance value is lower because the reactive power variations are not as large in the real world.

In [17], the estimated admittance matrices for the sequences zero and negative can also be found, which are not reported here. Note that the accuracy of estimated resistance and reactance for other sequences is highly dependent on load imbalance.

[8]Réseaux intelligents, French acronym for "Smart Grids".

[9]In one test scenario, we measured power and voltage magnitudes with another measurement device that has another power source, resulting in a more accurate estimate of the admittance matrix.

TABLE IV
ESTIMATED LINES PARAMETERS OF THE FIRST GRID (FIG. 4).

	$\hat{r}_{\mathrm{n}}^{(\mathrm{pos})}$ (Ohm)	$\hat{x}_{\mathrm{n}}^{(\mathrm{pos})}$ (Ohm)	diff (%)
L1	0.077946	0.072152	11.5987
L2	0.064411	0.064411	6.1523
L3	0.084847	0.069227	14.6247
L4	0.106323	0.076457	5.0064
L5	0.052123	0.062134	12.4726
L6	0.108537	0.072360	1.2836

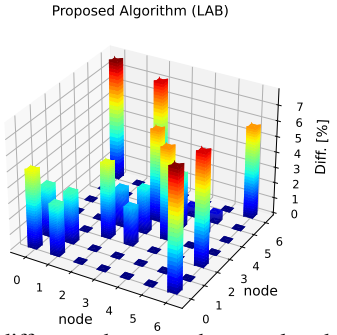

Fig. 8. Absolute difference between the actual and estimated admittance matrices by proposed method in laboratory.

C. Performance Assessment: Third Case "REAL"

We used ten-minute average measurements acquired during a month from 20/09/2019 to 19/10/2019 from a real-world distribution grid in Switzerland. With this one-month data, we were able to get a good approximation of the lines' resistance and reactance values. The ratio of training to testing data is assumed to be $5:1$; thus, 25 days of data are considered for training. The estimated resistance and the reactance of the grid's lines for positive, negative, and zero sequences are shown in Table V. Note that the estimated resistances of the lines are close to their nominal resistances; however, there is a difference between the estimated and nominal reactance values. The difference between measurement-based reactance and nominal reactance may be due to the fact that the lines are underground and the surrounding environment effects such as inductive coupling with other parallel wires or pipelines must be considered, whereas nominal reactance quantifies the reactance while excluding these effects.

TABLE V
ESTIMATED LINES PARAMETERS OF THE SECOND GRID (FIG. 5).

	L1	L2	L3	L4
$\hat{r}_{\mathrm{n}}^{(\mathrm{pos})}$ (Ohm)	0.018525	0.030595	0.061533	0.011633
$\hat{r}_{\mathrm{n}}^{(\mathrm{neg})}$ (Ohm)	0.012616	0.019504	0.037250	0.007460
$\hat{r}_{\mathrm{n}}^{(\mathrm{zero})}$ (Ohm)	0.017566	0.016984	0.025118	0.017818
$\hat{x}_{\mathrm{n}}^{(\mathrm{pos})}$ (Ohm)	0.012342	0.013592	0.022595	0.008708
$\hat{x}_{\mathrm{n}}^{(\mathrm{neg})}$ (Ohm)	0.006777	0.015167	0.026787	0.008581
$\hat{x}_{\mathrm{n}}^{(\mathrm{zero})}$ (Ohm)	0.009399	0.013925	0.034954	0.009440
diff (%)	34.64	32.75	26.96	62.04

We perform a load flow calculation on the testing data (the remaining 5 days of the data) to evaluate the performance of the estimated admittance matrix. The error $\delta_{\mathrm{n}}^{(\mathrm{s})}$

(the objective of problem (13)) is shown for the testing data in Table VI. It can be seen that the error of a load flow when using the estimated parameters is often lower than when using the nominal parameters. Moreover, the actual $\psi^{(\mathrm{s})}_{\mathrm{N2,t}} = (V^{(\mathrm{s})}_{\mathrm{N2,t}})^2 - (V^{(\mathrm{s})}_{\mathrm{up(N2),t}})^2$ is compared in Figs. 9 and 10, for $s \in \{\mathrm{pos}, \mathrm{zero}\}$, with $(\psi^{(\mathrm{s})}_{\mathrm{N2,t}})' = 2 \cdot \hat{r}^{(s)}_{\mathrm{N2}} \cdot \tilde{P}^{(\mathrm{s})}_{\mathrm{N2,t}} + 2 \cdot \hat{x}^{(s)}_{\mathrm{N2}} \cdot \tilde{Q}^{(\mathrm{s})}_{\mathrm{N2,t}} - ((\hat{r}^{(s)}_{\mathrm{N2}})^2 + (\hat{x}^{(s)}_{\mathrm{N2}})^2) \cdot (\tilde{I}^{(\mathrm{s})}_{\mathrm{N2,t}})^2$ using the lines nominal data and $(\psi^{(\mathrm{s})}_{\mathrm{N2,t}})'' = 2 \cdot r^{(s)}_{\mathrm{N2}} \cdot \tilde{P}^{(\mathrm{s})}_{\mathrm{N2,t}} + 2 \cdot x^{(s)}_{\mathrm{N2}} \cdot \tilde{Q}^{(\mathrm{s})}_{\mathrm{N2,t}} - ((r^{(s)}_{\mathrm{N2}})^2 + (x^{(s)}_{\mathrm{N2}})^2) \cdot (\tilde{I}^{(\mathrm{s})}_{\mathrm{N2,t}})^2$ using the estimated parameters of the lines. It is discovered that the proposed estimation leads to a better prediction of $\psi^{(\mathrm{s})}_{\mathrm{N2,t}}$. There are similar figures for other lines and sequences that are not depicted in this paper due to the page limitations. All of the figures and additional scenarios can be found on [17].

TABLE VI
ERROR $\delta^{(\mathrm{s})}_{\mathrm{n}}$ FOR THE TESTING DATA (IN %).

	s	N2	N3	N4	N5
Nominal	pos	9.47E-4	2.52E-4	1.37E-3	5.89E-4
Proposed method	pos	4.72E-4	1.58E-4	9.4E-4	2.76E-4
Nominal	zero	1.51E-7	3.71E-7	8.42E-7	2.87E-7
Proposed method	zero	1.35E-7	2.46E-7	1.15E-6	2.98E-7

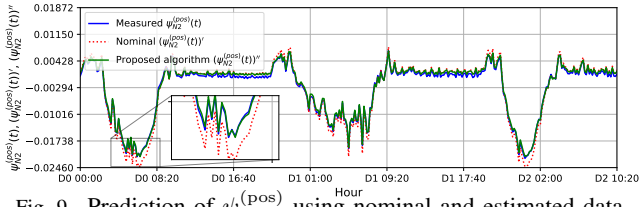

Fig. 9. Prediction of $\psi^{(\mathrm{pos})}_{\mathrm{N2,t}}$ using nominal and estimated data.

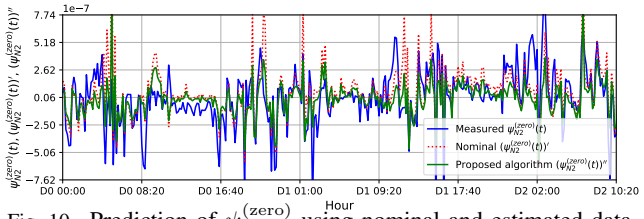

Fig. 10. Prediction of $\psi^{(\mathrm{zero})}_{\mathrm{N2,t}}$ using nominal and estimated data.

V. CONCLUSION

The paper proposes a method for estimating the admittance matrix of a three-phase radial distribution grid using data from low-cost measurement devices that only record ten-minute three-phase voltage magnitudes, active power, and reactive power with a certain level of precision. The proposed method is based on the distribution flow (DistFlow) model and solves a regression problem to determine the best-fitting DistFlow equations for the measurement data. The proposed method outperforms the state-of-the-art methods that use voltage phasors. This is more evident in the presence of measurement noise. In future works, the transversal elements of the grid's lines and transformers will be estimated using measurements of low-cost devices. Additionally, we intend to evaluate the robustness of our method under various operating scenarios and its applicability to larger distribution grids.

ACKNOWLEDGMENT

This research project is financially supported by the Swiss Innovation Agency Innosuisse.

REFERENCES

[1] M. Bozorg, N. Fatemi, C. A. Pena, O. Mousavi, and M. Carpita, "L'intelligence artificielle au service des réseaux: le projet grid data digger," *bulletin.ch, Fachzeitschrift und Verbandsinformationen von Electrosuisse und VSE, Bulletin SEV/AES: revue spécialisée et informations des associations Electrosuisse et AES*, 2020.

[2] I. Slutsker, S. Mokhtari, and K. Clements, "Method and apparatus for real time recursive parameter energy management system," Jan. 13 1998. US Patent 5,708,590.

[3] C. Wells, "Impedance measurement of a power line," July 13 2010. US Patent 7,755,371.

[4] M. Saadeh, R. McCann, M. Alsarray, and O. Saadeh, "A new approach for evaluation of the bus admittance matrix from synchrophasors:(a statistical Ybus estimation approach)," *International Journal of Electrical Power & Energy Systems*, vol. 93, pp. 395–405, Dec. 2017.

[5] O. Lateef, R. Harley, and T. Habetler, "Bus admittance matrix estimation using phasor measurements," in *2019 IEEE Power & Energy Society Innovative Smart Grid Technologies Conference (ISGT)*, pp. 1–5, IEEE, Feb. 2019.

[6] O. Ardakanian, V. Wong, R. Dobbe, S. Low, A. von Meier, C. Tomlin, and Y. Yuan, "On identification of distribution grids," *IEEE Transactions on Control of Network Systems*, vol. 6, no. 3, pp. 950–960, Jan. 2019.

[7] R. K. Gupta, F. Sossan, J.-Y. Le Boudec, and M. Paolone, "Compound admittance matrix estimation of three-phase untransposed power distribution grids using synchrophasor measurements," *IEEE Transactions on Instrumentation and Measurement*, vol. 70, pp. 1–13, 2021.

[8] V. L. Srinivas and J. Wu, "Topology and parameter identification of distribution network using smart meter and μpmu measurements," *IEEE Transactions on Instrumentation and Measurement*, vol. 71, pp. 1–14, 2022.

[9] X. Miao, M. Ilić, X. Wu, and U. Münz, "Distribution grid admittance estimation with limited non-synchronized measurements," in *2019 IEEE Power & Energy Society General Meeting (PESGM)*, pp. 1–5, IEEE, 2019.

[10] D. Flynn, A. B. Pengwah, R. Razzaghi, and L. L. Andrew, "An improved algorithm for topology identification of distribution networks using smart meter data and its application for fault detection," *IEEE Transactions on Smart Grid*, 2023.

[11] A. Amberg, A. Rangel, *et al.*, "Tutorial on symmetrical components," *Selinc. Cachefly. Net*, vol. 1, pp. 1–6, 2014.

[12] M. Baran and F. Wu, "Network reconfiguration in distribution systems for loss reduction and load balancing," *IEEE Power Engineering Review*, vol. 9, no. 4, pp. 101–102, April 1989.

[13] B. Gärtner and S. Schönherr, "An efficient, exact, and generic quadratic programming solver for geometric optimization," in *Proceedings of the sixteenth annual symposium on Computational geometry*, pp. 110–118, 2000.

[14] P. Virtanen, R. Gommers, T. E. Oliphant, M. Haberland, T. Reddy, D. Cournapeau, E. Burovski, P. Peterson, W. Weckesser, J. Bright, *et al.*, "Scipy 1.0: fundamental algorithms for scientific computing in python," *Nature methods*, vol. 17, no. 3, pp. 261–272, 2020.

[15] M. Carpita, J.-F. Affolter, M. Bozorg, D. Houmard, and S. Wasterlain, "Reine, a flexible laboratory for emulating and testing the distribution grid," in *2019 21st European Conference on Power Electronics and Applications (EPE'19 ECCE Europe)*, pp. P–1, IEEE, 2019.

[16] M. Carpita, A. Dassatti, M. Bozorg, *et al.*, "Low voltage grid monitoring and control enhancement: the grideye solution," in *2019 International Conference on Clean Electrical Power (ICCEP)*, pp. 94–99, IEEE, July 2019.

[17] M. Rayati, "Ybus Estimation Code." https://github.com/heig-vd-iese/ybus-estimation/blob/master/paper.ipynb, 07 2023.

[18] M. Shamshiri, C. K. Gan, and C. W. Tan, "A review of recent development in smart grid and micro-grid laboratories," in *2012 IEEE International Power Engineering and Optimization Conference Melaka, Malaysia*, pp. 367–372, IEEE, 2012.

[19] C. Patrascu, N. Muntean, O. Cornea, and A. Hedes, "Microgrid laboratory for educational and research purposes," in *2016 IEEE 16th international conference on environment and electrical engineering (EEEIC)*, pp. 1–6, IEEE, 2016.